ON THE STRUCTURE OF FUNCTION SPACES IN OPTIMAL RECOVERY OF POINT FUNCTIONALS FOR ENO-SCHEMES BY RADIAL BASIS FUNCTIONS

ARMIN ISKE AND THOMAS SONAR

January 15, 1996

ABSTRACT. Radial basis functions are used in the recovery step of finite volume methods for the numerical solution of conservation laws. Being conditionally positive definite such functions generate optimal recovery splines in the sense of Micchelli and Rivlin in associated native spaces. We analyse the solvability to the recovery problem of point functionals from cell average values with radial basis functions. Furthermore, we characterise the corresponding native function spaces and provide error estimates of the recovery scheme. Finally, we explicitly list the native spaces to a selection of radial basis functions, thin plate splines included, before we provide some numerical examples of our method.

CONTENTS

1991 *Mathematics Subject Classification.* 65M60 41A15 41A29 41A63; Secondary 65N30 76M25.
Key words and phrases. Optimal Recovery, Radial Basis Functions, Finite Volume Methods, ENO Schemes, Conservation Laws.

1. Introduction

In [29] the theory of optimal recovery as developed by Golomb & Weinberger [7] and Micchelli & Rivlin [20], [21], [22] was applied to the process of reconstructing a function from given cell averages in finite volume approximations of hyperbolic conservation laws. In the class of ENO-approximations studied in [29] the strict division between reconstructing a locally defined function from given cell averages and the evolution of this function in time not only makes the application of the theory of optimal recovery possible but also invites for doing so. The classical approach of piecewise discontinuous polynomial recovery was shown to be trivial in the light of optimal recovery and splines in semi-Hilbert spaces were identified as optimal. The multivariate generalisation of the classical cubic spline can be found as the thin plate spline in Beppo-Levi space and the construction of Beppo-Levi spline recoveries was exploited in detail. Since a result of Holladay-type holds for the thin plate spline it is optimal in its native function space. Numerical results indicated that the ENO-approximations using the thin plate spline recovery were much better behaved than the piecewise polynomial recovery and that numerical solutions showed higher accuracy.

In a general setting we are concerned with a set of values of linear functionals $L_i u \in \mathbb{R}$, $i = 0, \ldots, M-1$, of an unknown function $u : \mathbb{R}^d \to \mathbb{R}$ which is a member of a Banach space V. We seek an optimal approximation to the value of yet another linear functional Λu. We assume that the approximation to Λu can be computed from the knowledge of the M values $L_i u$. If the linear functionals L_i are considered as an entity, the vector

$$\mathfrak{I}u := (L_0 u, \ldots, L_{M-1} u) \in \mathbb{R}^M$$

is called the *information* available for Λ. The linear functional Λ is called the *feature operator*. Any (not necessarily linear) operator $\mathfrak{R}$ with the property

$$\mathfrak{R} : \mathfrak{I}u \to \mathbb{R}$$

is called *recovery operator* or *recovery algorithm*. It was already observed by Golomb and Weinberger in [7], that knowledge of M linearly independent linear functionals does not suffice to recover another linear functional which is linearly independent from each of the M given ones. Thus, a nonlinear constraint is needed. To establish this constraint we call a linear operator

$$\mathfrak{T} : V \to V$$

a *restriction operator* and define a convex, balanced, and absorbing subset U of V by

$$U := \{v \in V \ : \ \|\mathfrak{T}v\|_V \leq 1\}.$$

Operators and spaces involved in recovery are shown in figure 1. If the restriction is taken to be the identity operator on V the set U is the unit sphere in V. In contrast, if we specify on Hilbert spaces, the information $\mathfrak{I}u$ defines a hyperplane in V and if the recovery problem is solvable at all then sphere and hyperplane intersect and constitute a hypercircle in the sense of Prager and Synge [30]. The centre $z(u)$ of the hypercircle is

$$\begin{tikzcd}
U \subset V \arrow[r, "\Lambda"] \arrow[d, "\mathfrak{I}"'] & \mathbb{R} \\
\mathbb{R}^M \arrow[ur, "\mathfrak{R}"'] &
\end{tikzcd}$$

FIGURE 1. Operators and spaces in the theory of optimal recovery

the point with least distance to all other points on the circle and thus, as was concluded already by Golomb and Weinberger, $\Lambda z(u)$ is the best approximation to Λu.

The geometric ideas just presented can be formalised to result in a general theory of recovery as developed by Micchelli and Rivlin, [20], [21], [22]. A short but sufficiently complete overview was given in [29]. Associated with each recovery operator is an error

$$E_{\mathfrak{R}}(\Lambda, \mathfrak{I}, U) := \sup_{u \in U}\{|\Lambda u - \mathfrak{R}\mathfrak{I}u|\}.$$

The quantity

$$E(\Lambda, \mathfrak{I}, U) := \inf_{\mathfrak{R}} E_{\mathfrak{R}}(\Lambda, \mathfrak{I}, U)$$

is called the *intrinsic error*. Consequently, an operator $\mathfrak{R}^*$ is called *optimal recovery operator*, if

$$E_{\mathfrak{R}^*}(\Lambda, \mathfrak{I}, U) = E(\Lambda, \mathfrak{I}, U) = \inf_{\mathfrak{R}} \sup_{u \in U}\{|\Lambda u - \mathfrak{R}\mathfrak{I}u|\}$$

holds. Now let V be a semi-Hilbert space with bilinear form $[\cdot|\cdot]_V$ and corresponding seminorm $|\cdot|$. The set $A(u) := \{v \in V \mid \mathfrak{I}v = \mathfrak{I}u\}$ contains all functions which identically have the same information as the unknown function u. We call a function $\Phi \in A(u)$ a *recovery spline*, if a generalised Holladay-type result

$$|\mathfrak{T}\Phi|_V = \min_{v \in A(u)} |\mathfrak{T}v|_V$$

holds for this function. It can be shown that recovery splines constitute the optimal recovery algorithms in their associated semi-Hilbert spaces, see [31] or [29], which we refer throughout this paper as *native spaces*, and the optimal spline recovery algorithm given by

$$\mathfrak{R}^*\mathfrak{I}u = \Lambda\Phi.$$

Thus, Φ is the centre of the aforementioned hypercircle.

In this paper we ask for recovery splines of the general form

$$s(x) := \sum_{j=0}^{M-1} \lambda_j L_j^y \psi(x-y) + \sum_{\ell=0}^{Q-1} \beta_\ell p_\ell(x), \tag{1.1}$$

where $\{p_0, \dots, p_{Q-1}\}$ form a basis of $\Pi_m(\mathbb{R}^d)$, being the linear space of all d-variate polynomials of order not exceeding m, i. e. $Q = \binom{m-1+d}{d}$, and $\psi : \mathbb{R}^d \to \mathbb{R}$ is referred as *basis function*. A possible choice for ψ could be any of the following *radial basis functions* that we list here for reasons of convenience and easy reference together with a lower estimate for the order m of the polynomial part to be augmented:

Radial basis function	$\psi(x) =$	$m \in \mathbb{N}_0$
polynomials	$\lvert x\rvert^\nu, \nu > 0, \nu \notin 2\mathbb{N}$	$m > \nu/2$
thin plate splines	$\lvert x\rvert^{2k} \log \lvert x\rvert, k \in \mathbb{N}$	$m > k$
Gaussians	$e^{-\alpha\lvert x\rvert^2}, \alpha > 0$	$m \geq 0$
multiquadrics	$(c^2 + \lvert x\rvert^2)^{\nu/2}, \nu > 0, \nu \notin 2\mathbb{N}$	$m > \nu/2$
inverse multiquadrics	$(c^2 + \lvert x\rvert^2)^{\nu/2}, -d < \nu < 0, \nu \notin 2\mathbb{Z}$	$m \geq 0$

As can be seen the Gaussians as well as the inverse multiquadrics do not require a polynomial part in the recovery spline which makes them very attractive for recovery in finite volume approximations.

The coefficients $\lambda_j, j = 0, \dots, M-1$, and $\beta_j, j = 0, \dots, Q-1$, are determined through the fundamental recovery conditions

$$L_j s = L_j u \qquad 0 \leq j \leq M-1$$

plus Q side conditions to be specified later. In view of our application, a few questions arise quite naturally:

- Given ψ, does there exist a solution of the recovery problem and is a possible solution unique?
- What are the function spaces in which the general recovery spline is optimal?
- Can one provide local error estimates of the recovery algorithm?

The plan of the paper is the following: In section 2 the practical background of our work, namely the recovery of point functionals from cell averages in finite volume ENO-approximations to hyperbolic conservation laws is described. In [19] conditions were given on functions of the form (1.1) in the case $L_i \equiv \delta_{x_i}$, i.e. the case of interpolation at scattered nodes, in order to prove solvability of the interpolation problem. Section 3 is devoted to show that the general theory as developed in [12] can be applied to our recovery problem. Therefore, the notion of conditional positive definiteness plays a key role. In section 4 we construct explicitly the *native spaces* in which our recovery algorithm given by a function of the form (1.1) is optimal. Since possible error functionals are continuous on the corresponding native space, this enables us to provide local error estimates for our method. Finally, section 5 contains the description of a finite volume ENO-method and several numerical examples.

2. Finite volume approximations

2.1. The governing equations. We consider conservation laws

$$\partial_t u + \sum_{\ell=1}^{d} \partial_{x_\ell} f_\ell(u) = 0 \tag{2.1}$$

for functions $\mathbb{R}^d \times \mathbb{R}^+ \ni (x,t) \stackrel{u}{\longmapsto} u(x,t) \in \Sigma \subset \mathbb{R}^n$ where the flux functions $f_\ell : \Sigma \to \mathbb{R}^n$ are assumed to be smooth. The open set Σ is called *state space*. We assume the systems to be hyperbolic in the following sense. The matrix

$$A(u,\nu) := \sum_{\ell=1}^{d} \nabla_u f_\ell(u)\nu_\ell,$$

where $\nabla_u f_\ell$ denotes the Jacobian matrix of f_ℓ with respect to u, exhibits exactly n real eigenvalues $\lambda_j, j = 1, \dots, n$ and thus is diagonalisable for all vectors $\nu = (\nu_1, \dots, \nu_d) \in \mathbb{R}^d$. It is well-known (see [13]) that discontinuities develop naturally after finite time and solutions can only be understood in the weak sense. Instead of utilising a notion of weak solutions depending on test functions we test an integral form of the conservation law on a class of bounded subsets of $\mathbb{R}^d$ which we call control volumes. For our purposes a control volume can be defined as a bounded domain $\sigma \subset \mathbb{R}^d$ with Lipschitz continuous boundary $\partial\sigma$. This assumption guarantees the existence of the outer unit normal vector $n = (n_1, \dots, n_d)^T \in \mathbb{R}^d$ at $\partial\sigma$ in the classical sense. In a more general setting control volumes may exhibit even fractal boundaries in which case notions from geometric measure theory [5] have to be used to define a normal vector properly.

Definition 2.1. A function $u \in L^1 \cap L^\infty(\mathbb{R}^d \times \mathbb{R}^+; \mathbb{R}^n)$ is called *weak solution* of the system (2.1), if

$$\frac{d}{dt}\int_\sigma u\,dx + \oint_{\partial\sigma} \sum_{\ell=1}^d f_\ell(u) n_\ell \, do = 0$$

holds on every control volume $\sigma \subset \mathbb{R}^d$.

It is worth noting that this definition is essentially equivalent to the test function-based notion of weak solutions. This was shown by Bruhn in [1] and, in another context, in earlier work by Morrey [23].

It is well known that weak solutions fail to be unique, see [28], and additional side conditions are needed to characterise a unique, physically correct, weak solution. The nature of such side conditions in the case of general hyperbolic conservation laws is still not clear, see [26], but it is hoped that entropy inequalities are useful at least for those systems which directly model a physical system.

In order to give meaning to the definition of weak solutions we introduce an integral operator on each control volume.

Definition 2.2. If $u \in L^1 \cap L^\infty(\mathbb{R}^d \times \mathbb{R}^+; \mathbb{R}^n)$ is a weak solution of a hyperbolic conservation law and $\sigma \subset \mathbb{R}^d$ denotes a control volume, then the operator

$$\mathfrak{A}(\sigma) : \begin{cases} L^1 \cap L^\infty(\mathbb{R}^d \times \mathbb{R}^+; \mathbb{R}^n) & \longrightarrow \quad L^1 \cap L^\infty(\mathbb{R}^+; \mathbb{R}^n) \\ \hfill u & \longmapsto \quad \mathfrak{A}(\sigma)u(t) := \frac{1}{|\sigma|}\int_\sigma u(x,t)\,dx \end{cases}$$

is called *cell average operator* on σ.

Obviously, $\frac{d}{dt}\int_\sigma u(x,t)\,dx = |\sigma|\frac{d}{dt}\mathfrak{A}(\sigma)u(t)$, and thus the definition of weak solutions immediately leads to an evolution equation for cell averages.

Lemma 2.1. *Cell averages of weak solutions satisfy the evolutionary system*

$$\frac{d}{dt}\mathfrak{A}(\sigma)u(t) = -\frac{1}{|\sigma|}\oint_{\partial\sigma} \sum_{\ell=1}^d f_\ell(u) n_\ell \, do \tag{2.2}$$

on each control volume $\sigma \subset \mathbb{R}^d$.

Since the numerical methods we are interested in are directly based on this evolutionary system, this will be the form of equations on which we want to concentrate.

To be more specific on the type of systems we want to consider, the Euler equations of inviscid, compressible fluids are introduced in $d = 2$ space dimensions. If $\rho, v = (v_1, v_2)^T, p$ and E denote density, velocity, pressure and total energy of a fluid, the vector of conservative variables and the fluxes are given by

$$u = \begin{bmatrix} \rho \\ \rho v_1 \\ \rho v_2 \\ \rho E \end{bmatrix}, \quad f_\ell(u) = \begin{bmatrix} \rho v_\ell \\ \rho v_1 v_\ell + \delta_1^\ell p \\ \rho v_2 v_\ell + \delta_2^\ell p \\ \rho H v_\ell \end{bmatrix},$$

where $H := E + p/\rho$ denotes enthalpy and δ_i^ℓ is the Kronecker's delta. Inspection of the Jacobian matrices shows that the Euler equations are hyperbolic and that the eigenvalues of $A(u, \nu)$ are given by

$$\lambda_1 = v^T \nu - a|\nu|, \quad \lambda_2 = \lambda_3 = v^T \nu, \quad \lambda_4 = v^T \nu + a|\nu|,$$

where $a := \sqrt{\kappa p/\rho}$ denotes the speed of sound and κ the ratio of specific heats, which is $\kappa = 1.4$ for dry air.

As they stand, the Euler equations in two space dimensions constitute a hyperbolic system of four equations of conservation laws for the five unknowns ρ, v_1, v_2, p and E. Thus, one further closure condition is needed and found in the equation of state, which, for ideal gases, is given by

$$p = (\kappa - 1)\rho \left(E - \frac{1}{2}|v|^2 \right).$$

2.2. Finite volume approximations on triangulations. Suppose the solution to a hyperbolic system of conservation laws is sought on a bounded subset $\overline{\Omega} \subset \mathbb{R}^d$, on which a conforming triangulation can be established. For simplicity only the boundary of $\overline{\Omega}$ is assumed to be polygonal.

Definition 2.3. A *triangulation* $\mathcal{T}^h$ of $\overline{\Omega}$ is a subdivision of $\overline{\Omega}$ into finitely many subsets $T_i \subset \overline{\Omega}, i = 1, \ldots, \#T$, such that the following conditions are satisfied.

- $\overline{\Omega} = \bigcup_{i \in \{1,\ldots,\#T\}} T_i$.
- Every $T_i \in \mathcal{T}^h$ is closed and the interior $\mathring{T}_i$ is nonempty.
- For each pair $T_i, T_j \in \mathcal{T}^h$ with $i \neq j$ it holds that $\mathring{T}_i \cap \mathring{T}_j = \emptyset$.
- Every $T_i \in \mathcal{T}^h$ has a Lipschitz continuous boundary.

A triangulation is *conforming*, if additionally the following condition is satisfied.

- Every $(d-1)$-dimensional face of any $T_i \in \mathcal{T}^h$ does either belong to the boundary $\partial\overline{\Omega}$ or is the face of another $T_j \in \mathcal{T}^h, i \neq j$.

Note that h corresponds to a typical one-dimensional geometrical measure of the triangulation, for example, the largest diameter of all T_i's.

For simplicity and ease of computation we further specify the type of elements T_i of a triangulation. We call a conforming triangulation a *primary grid*, if all $T_i \in \mathcal{T}^h$ are d-simplices, i.e. triangles in two, tetrahedrons in three space dimensions.

Definition 2.4. If $T_i \in \mathcal{T}^h$ denotes a d-simplex, then

$$N(i) := \{j \in \mathbb{N} \mid T_i \cap T_j \text{ is face of } T_i\}.$$

If each of the simplices T_i is considered as a control volume, the evolution equation of cell averages (2.2) on T_i is given by

$$\frac{d}{dt}\mathfrak{A}(T_i)u(t) = -\frac{1}{|T_i|}\sum_{j\in N(i)}\int_{\partial T_i\cap\partial T_j}\sum_{\ell=1}^{d} f_\ell(u)n_{ij,\ell}\,do,$$

$n_{ij} = (n_{ij,1}, \ldots, n_{ij,d})^T$ denoting the outer unit normal vector on the face $\partial T_i \cap \partial T_j$. For the interesting cases $d = 2$ and $d = 3$ the integral on the right hand side is a line integral and a surface integral, respectively. Utilising a mapping

$$x_{ij} : \left\{ \begin{array}{ccl} S & \longrightarrow & \partial T_i \cap \partial T_j \\ s & \longmapsto & x(s) \end{array} \right.$$

from a parameter space S onto $\partial T_i \cap \partial T_j$ the evolution equation can be rewritten to give

$$\frac{d}{dt}\mathfrak{A}(T_i)u(t) = -\frac{1}{|T_i|}\sum_{j\in N(i)} D(|\partial T_i \cap \partial T_j|)\int_S \sum_{\ell=1}^{d} f_\ell(u(x_{ij}(s),t))n_{ij,\ell}\,ds,$$

such that $D(|\partial T_i \cap \partial T_j|)$ denotes a certain multiple of the volume (length, area) of $\partial T_i \cap \partial T_j$ while $|S| = \mathcal{O}(1)$. In two space dimensions S can be chosen to be the interval $[-1, 1]$ while for $d = 3$ S is a unit triangle with fixed coordinates of its edge points.

Suppose that a quadrature rule of the form

$$\int_S g(x(s))\,ds = \sum_{\nu=1}^{N}\omega_\nu g(x(s_\nu)) + \mathcal{O}(h^q)$$

is available, where N denotes the number of integration points and ω_ν certain quadrature weights. Assuming smooth solutions u this allows to write

$$\frac{d}{dt}\mathfrak{A}(T_i)u(t) = -\frac{1}{|T_i|}\sum_{j\in N(i)} D(|\partial T_i \cap \partial T_j|)\left\{\sum_{\nu=1}^{N}\omega_\nu\sum_{\ell=1}^{d} f_\ell(u(x_{ij}(s_\nu),t))n_{ij,\ell} + \mathcal{O}(h^q)\right\}.$$

To be capable of capturing discontinuous solutions requests an algorithmic device which we take from finite difference methods, see [**?**].

Definition 2.5. A mapping

$$H : \left\{ \begin{array}{ccl} \mathbb{R}^n \times \mathbb{R}^n \times \mathbb{R}^d & \longrightarrow & \mathbb{R}^n \\ (v, w, n) & \longmapsto & H(v, w; n) \end{array} \right.$$

is called *numerical flux function* or *approximate Riemann solver*, if it is consistent in the sense of

$$\forall w \in \mathbb{R}^n \quad \forall n \in \mathbb{R}^d : \quad H(w, w; n) = \sum_{\ell=1}^{d} f_\ell(w)n_\ell.$$

If we now assume smooth solutions again a numerical flux function can be introduced without difficulty to result in

$$\frac{d}{dt}\mathfrak{A}(T_i)u(t) = -\frac{1}{|T_i|}\sum_{j\in N(i)} D(|\partial T_i \cap \partial T_j|)\left\{\sum_{\nu=1}^{N}\omega_\nu H\left(u(x_{ij}(s_\nu),t), u(x_{ij}(s_\nu),t); n_{ij}\right) + \mathcal{O}(h^q)\right\}.$$

Note that still weak solutions are used in this formulation. With the following definition basic finite volume approximations are introduced.

Definition 2.6. The numerical method: For given $t^* > 0$ find $\overline{u}(t^*)$ for each $T_i, i = 1, \ldots, \#T$, as solution of the ordinary initial value problem

$$\begin{aligned}\frac{d}{dt}\overline{u}(t)|_{T_i} &= -\frac{1}{|T_i|}\sum_{j\in N(i)} D(|\partial T_i \cap \partial T_j|)\omega_1 H\left(\overline{u}(t)|_{T_i}, \overline{u}(t)|_{T_j}; n_{ij}\right)\\ \overline{u}(0)|_{T_i} &= \mathfrak{A}(T_i)u(0),\end{aligned}$$

is called *basic finite volume approximation.*

Note that a one-point quadrature rule was chosen although there is no choice of quadrature point (any point on $\partial T_i \cap \partial T_j$ is a valid quadrature point). Nevertheless, the weight ω_1 may be a number not equal to one, depending on the choice of S. Note that the best possible order attainable with a one-point rule is $q = 2$.

If we agree on calling a basic finite volume approximation of k-th order in space if

$$\omega_1 H\left(\overline{u}(t)|_{T_i}, \overline{u}(t)|_{T_j}; n_{ij}\right) = \int_S \sum_{\ell=1}^{d} f_\ell(u(x_{ij}(s),t))n_{ij,\ell}\, ds + \mathcal{O}(h^k),$$

then the following theorem holds true.

Theorem 2.1. *If u as well as H are sufficiently smooth, then the basic finite volume approximation is first order accurate in space.*

The proof of this theorem is easily accomplished by Taylor series development around a quadrature point on $\partial T_i \cap \partial T_j$. The poor approximation property

$$\mathfrak{A}(T_i)u(t) = u(x(s_1),t) + \mathcal{O}(h)$$

of the cell average operator at the quadrature point – also easily provable by means of Taylor expansion – is then the dominating source of inaccuracy, even though a one-point quadrature rule may lead to second order accurate integration. Once this source of error is detected, the principle of constructing high order accurate finite volume methods is readily visible.

Definition 2.7. If for fixed $t \geq 0$ on $T_i \in \mathcal{T}^h$ the smooth function

$$s_u^i : \begin{cases} T_i \times \mathbb{R}^+ & \longrightarrow \quad \mathbb{R}^n \\ \quad (x,t) & \longmapsto \quad s_u^i(x,t)\end{cases}$$

satisfies the two conditions

$$(s_u^i - u)(x,t) = \mathcal{O}(h^r), \quad r > 0, x \in T_i \tag{2.3}$$

$$\mathfrak{A}(T_i)s_u^i(t) = \mathfrak{A}(T_i)u(t), \tag{2.4}$$

then the ordinary initial value problem

$$\begin{aligned}\frac{d}{dt}\overline{u}(t)|_{T_i} &= -\frac{1}{|T_i|}\sum_{j\in N(i)} D(|\partial T_i \cap \partial T_j|)\sum_{\nu=1}^{M}\omega_\nu H\left(s_u^i(x_{ij}(s_\nu),t), s_u^j(x_{ij}(s_\nu),t); n_{ij}\right)\\ \overline{u}(0)|_{T_i} &= \mathfrak{A}(T_i)u(0)\end{aligned}$$

is called *finite volume approximation.* The function s_u^i is called *recovery function* on T_i.

We remark that basic finite volume approximations are included in this definition as the special case $s_u^i \equiv \mathfrak{A}(T_i)u$. In that case $r = 1$ holds due to the aforementioned poor approximation properties of the cell average operator. If we now call a finite volume method of k-th order in space if

$$\sum_{\nu=1}^{M}\omega_\nu H\left(s_u^i(x_{ij}(s_\nu),t), s_u^j(x_{ij}(s_\nu),t); n_{ij}\right) = \int_S \sum_{\ell=1}^{d} f_\ell(u(x_{ij}(s),t))n_{ij,\ell}\,ds + \mathcal{O}(h^k),$$

then it is easily seen that the following theorem is valid, see [29].

Theorem 2.2. *If the order of accuracy of the quadrature rule is $\mathcal{O}(h^q)$ and if $(s_u^i - u)(x,t) = \mathcal{O}(h^r), r > 0$, holds on $T_i \in \mathcal{T}^h$, then the finite volume approximation is of order $\mathcal{O}(h^{\min\{q,r\}})$ in space, provided u as well as H are smooth enough functions.*

Thus, if recovery functions can be computed on each $T_i \in \mathcal{T}^h$, then a quadrature rule can be found such that the order condition (2.3) determines the spatial order of a finite volume method.

2.3. Node sets and ENO methods. In the construction of higher order finite volume schemes we are faced with at least two main practical problems. The first one is concerned with the choice and selection of stencils used for the construction of recovery functions on T_i and, secondly, the problem of handling discontinuous data. The second problem can be circumvented using the ENO (Essentially Non-Oscillatory) approach, see [8], [29]. We agree on accepting a recovery function s_u^i on T_i only if its oscillatory behaviour is not too bad in a sense to be specified. Accepting an oscillatory recovery function leads to new extrema in the numerical solution (which is unphysical) and can cause values of the variables outside the state space Σ which, in turn, may cause disastrous effects (for instance, if density or pressure get negative values in a flow field). Therefore a whole set of recovery functions for simplex T_i is needed from which one can choose the least oscillating one and assign it to T_i.

We recover by using M values $\overline{u}_i(t), i = 0,\ldots,M-1$, where $\overline{u}_i(t) := \overline{u}(t)|_{T_i}$. Thus, $\overline{u}_0,\ldots,\overline{u}_{M-1}$ are cell averages on simplices in a certain neighborhood of T_i.

Definition 2.8. Every set of pairwise distinct control volumes

$$K(T_i) := \{T_i, T_{i_1}, \ldots, T_{i_{M-1}}\}$$

is called *node set* for T_i.

In principle, the cardinality of node sets may vary from simplex to simplex. For the sake of simplicity of the resulting algorithms we assume the cardinality of each node set to be exactly M.

The algorithmic part concerning the choice of node sets usually is called *stencil selection scheme*, see [8]. One idea for stencil selection which seems to be attractive at first glance is a recursive search for paths through the grid, which pass through T_i and have length (in the sense of number of simplices) M. Albeit the simplicity of this idea the resulting stencil selection scheme turns out to be unusable. Even small M in space dimension $d = 2$ result in thousands of valid node sets such that the run-time of the overall finite volume algorithm is unacceptable.

Several strategies were therefore developed in the literature ranging from a fixed stencil selection to recursive sector search algorithms, see [8], [32], [29]. We adopt the approach presented in [29] and choose a set of four stencils, one corresponding to a central difference while the remaining three stencils correspond to upwind stencils according to figure 2. Thus, each triangle is associated with four node sets containing four triangles each. Note

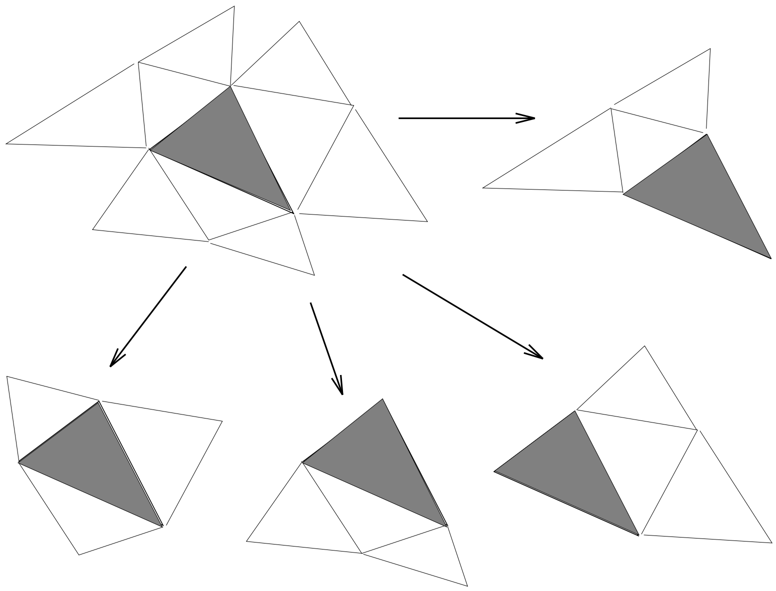

FIGURE 2. The construction of four node sets out of a certain neighbourhood

that there may be a loss of information at boundary triangles.

3. Recovery splines

3.1. Radial recovery. For the rest of this paper we fix the time variable $t \geq 0$ and consider a fixed simplex $T \in \mathcal{T}^h$ such that we drop its corresponding index i for reasons of notational simplicity. Note, that the cell average operator $\mathfrak{A}(T)$ is a vector of n linear functionals. Since each of the components is treated separately in the recovery process, we assume throughout this section that u is a real valued function.

Thus, with $T_0 := T$ on each node set

$$K(T) := \{T_0, T_1, \ldots, T_{M-1}\}$$

the linear functionals

$$L_j := \mathfrak{A}(T_j), \quad j = 0, \ldots, M-1,$$

constitute the information

$$\mathfrak{I}u := (L_0 u, \ldots, L_{M-1} u)$$

available for the feature operator

$$\Lambda_j := \delta_{x_j},$$

which is the Dirac functional located at a quadrature point x_j lying in $\partial T_0 \cap \partial T_j$, $j \in N(0)$. Our aim is to recover $u(x_j, t) = \langle \Lambda_j, u \rangle = \langle \delta_{x_j}, u \rangle$ from the given information $\mathfrak{I}$. As was already indicated in the introduction we are looking for a radial recovery function of the form

$$s(x) = \sum_{j=0}^{M-1} \lambda_j L_j^y \psi(x-y) + \sum_{\ell=0}^{Q-1} \beta_\ell p_\ell(x)$$

such that the recovery conditions

$$L_j s = L_j u, \quad j = 0, \ldots, M-1, \tag{3.1}$$

hold with a radial basis function $\psi : \mathbb{R}^d \to \mathbb{R}$ and a basis $p_0, \ldots, p_{Q-1}$ of $\Pi_m(\mathbb{R}^d)$. We aim at generalising results in [29] and therefore, the dependence on time is omitted since recovery has to be done on each fixed time level.

3.2. Well-posedness of the recovery problem. Now, we examine the solvability of the recovery problem from cell average values. Therefore, an important notion is that of conditional positive definiteness.

Definition 3.1. A function $\psi \in C(\mathbb{R}^d)$ is conditionally positive definite of order m on $\mathbb{R}^d$, if for all sets $X = \{x_0, \ldots, x_{M-1}\} \subset \mathbb{R}^d$ containing pairwise distinct points and all vectors $\lambda = (\lambda_0, \ldots, \lambda_{M-1}) \in \mathbb{R}^M \setminus \{0\}$ with

$$\sum_{j=0}^{M-1} \lambda_j p(x_j) = 0 \qquad \text{for all } p \in \Pi_m(\mathbb{R}^d) \tag{3.2}$$

the quadratic form

$$\sum_{i=0}^{M-1} \sum_{j=0}^{M-1} \lambda_i \lambda_j \psi(x_i - x_j)$$

is strictly positive.

Following [12] we assume that the basis function ψ possesses a *generalised Fourier transform* in the sense of the following definition.

Definition 3.2. The function $\psi : \mathbb{R}^d \to \mathbb{R}$ has a *generalised Fourier transform* $\varphi \in C(\mathbb{R}^d \setminus \{0\})$ if there is a number $k \in \mathbb{N}_0$, here assumed to be minimal with the property $\|\omega\|^k \varphi(\omega) \in L_1(0)$, such that Parseval's identity generalised as

$$\int_{\mathbb{R}^d} \psi(x)\gamma(x)\,dx = (2\pi)^{-d} \int_{\mathbb{R}^d} \varphi(\omega)\hat{\gamma}(\omega)\,d\omega \tag{3.3}$$

holds for all functions γ from

$$\mathcal{S}_k^\perp := \left\{ \gamma \in \mathcal{S} \,:\, \int \gamma(x)p(x)\,dx = 0 \text{ for all } p \in \Pi_k(\mathbb{R}^d) \right\}.$$

In the above definition,

$$\mathcal{S} := \left\{ \gamma \in C^\infty(\mathbb{R}^d, \mathbb{R}) : \lim_{|x|\to\infty} x^p D^q \gamma(x) = 0 \text{ for all } p, q \in \mathbb{N}_0^d \right\}$$

denotes the well-known *Schwartz space* containing all rapidly decreasing functions that have derivatives up to an arbitrary order. In addition, note that the Fourier transform

$$\hat{\gamma}(\omega) := \int_{\mathbb{R}^d} e^{-ix^T\omega} \gamma(x)\, dx$$

to each function $\gamma \in \mathcal{S}_k^\perp$ possesses a zero of order at least k at zero, which makes the integral on the right hand side of (3.3) well-defined. It comes out that all radial basis functions which appeared in our introduction possess a generalised Fourier transform (cf. [14], [25], [10]) which are strictly positive on all of $\mathbb{R}^d \setminus \{0\}$. However, as was proven in [10] for the conditional positive definiteness of ψ it suffices that $\varphi \not\equiv 0$ is nonnegative on all of $\mathbb{R}^d$. Exploiting this observation this leads to the required sufficient condition for ψ under which the solution of the recovery of cell average values has a unique solution.

Theorem 3.1. *Let ψ be conditionally positive definite of order m on $\mathbb{R}^d$ and assume that ψ possesses a generalised Fourier transform $\varphi \in C(\mathbb{R}^d \setminus \{0\})$. Then, the recovery problem* (3.1) *has a solution under constraints* (3.2) *which is unique provided that the information $\mathfrak{I}$ is injective on $\Pi_m(\mathbb{R}^d)$:*

$$L_j p = 0, \quad 0 \le j \le M-1 \quad \Longrightarrow \quad p \equiv 0 \qquad \textit{for all } p \in \Pi_m(\mathbb{R}^d). \tag{3.4}$$

Note, that for the special case $L_j = \delta_{x_j}$ the above theorem specialises to the multivariate interpolation problem to finitely many data where the existence and uniqueness of a solution have been established in a fundamental paper [19] by C.A. Miccelli. Hence, our proof is straight along the lines.

Proof. The reconstruction problem can be rewritten as a system of linear equations

$$\begin{bmatrix} A_{\psi,\mathfrak{I}} & P_{\mathfrak{I}} \\ P_{\mathfrak{I}}^T & 0 \end{bmatrix} \begin{bmatrix} \lambda \\ \beta \end{bmatrix} = \begin{bmatrix} \mathfrak{I}u \\ 0 \end{bmatrix}$$

where the block matrices are $A_{\psi,\mathfrak{I}} := (L_i^x L_j^y \psi(x-y))_{0\le i,j\le M-1}$ and $P_{\mathfrak{I}} := (L_i p_j)_{\substack{0\le i\le M-1 \\ 0\le j\le Q-1}}$. The entries λ and β correspond to the coefficient vectors $\lambda = (\lambda_0, \ldots, \lambda_{M-1})^T$ and $\beta := (\beta_0, \ldots, \beta_{Q-1})$. If we seek a solution of the corresponding homogeneous system we obtain

$$\begin{aligned} A_{\psi,\mathfrak{I}}\lambda + P_{\mathfrak{I}}\beta &= 0 \\ P_{\mathfrak{I}}^T \lambda &= 0 \end{aligned}$$

and thus

$$\lambda^T A_{\psi,\mathfrak{I}} \lambda + \underbrace{\lambda^T P_{\mathfrak{I}}}_{=0} \lambda = 0,$$

which is required to be true iff $\lambda = 0$. Indeed, since from (3.3) we conclude as in [12] that

$$\sum_{i,j=0}^{M-1} \lambda_i \lambda_j L_i^x L_j^y \psi(x-y) = (2\pi)^{-d} \int_{\mathbb{R}^d} |\chi_{\lambda,\mathfrak{I}}(\omega)|^2 \varphi(\omega)\, d\omega \tag{3.5}$$

holds, where the right hand side contains the *symbol function*

$$\chi_{\lambda,\Im}(\omega) = \sum_{j=0}^{M-1} \lambda_j L_j^x e^{-ix^T\omega}.$$

Now, since φ is nonnegative but not identically vanishing, the right hand side vanishes iff $\chi_{\lambda,\Im}$ vanishes on an open nonempty subset of $\mathbb{R}^d$. In this case, due to its analyticity $\chi_{\lambda,\Im}$ vanishes on all of $\mathbb{R}^d$ such that $\lambda_j = 0$ for $0 \le j \le M-1$ follows from the linear independence of $L_0, \ldots, L_{M-1}$. Finally, $\beta = 0$ follows from (3.4). Hence, the homogeneous system only allows the trivial solution. □

4. Error estimates and native spaces

Once the existence and uniqueness of a solution to the recovery problem is established one naturally asks for error estimates of the form

$$|s(x) - u(x)| \le C_u P_{\psi,\Im}(x), \tag{4.1}$$

where $x \in \Omega \subset \mathbb{R}^d$ is fixed, C_u denotes a positive constant depending on u and $P_{\psi,\Im}$ is referred as *power function*, which is to be understood as the norm of a possible error functional ϵ_x . Following Wu & Schaback [34] we provide a suitable representation of the error functional by

$$\epsilon_x = \delta_x - \sum_{j=0}^{M-1} v_j(x) L_j$$

where $v_0(x), \ldots, v_{M-1}(x)$ are real numbers with

$$p(x) = \sum_{j=0}^{M-1} v_j(x) L_j p \qquad \text{for all } p \in \Pi_m(\mathbb{R}^d)$$

such that the error functional ϵ_x is in the space

$$\Pi_m^\perp := \left\{ \lambda = \sum_{j=0}^{M-1} \lambda_j T_j \,:\, T_j \text{ comp. supp. }, \; T_0, \ldots, T_{M-1} \text{ lin. indep. }; \Pi_m(\mathbb{R}^d) \subset \ker \lambda \right\}$$

containing all finite linear combinations of compactly supported linear functionals which are orthogonal on each polynomial from $\Pi_m(\mathbb{R}^d)$. As it was proven in [12] for any $\lambda \in \Pi_m^\perp$ the identity (3.5) can be generalised as

$$\lambda^x \lambda^y \psi(x-y) = (2\pi)^{-d} \int_{\mathbb{R}^d} \varphi(\omega) |\lambda^x e^{-ix^T\omega}|^2 \, d\omega$$

provided that λ yields a well-defined left hand side. Obviously, all functionals λ with this property form a linear subspace $\Pi_\psi^\perp$ of $\Pi_m^\perp$ which is naturally equipped with the inner product

$$(\lambda, \mu)_\psi := \mu^x \lambda^y \psi(x-y), \qquad \text{for all } \lambda, \mu \in \Pi_\psi^\perp,$$

defining a corresponding norm $\|\cdot\|_\psi$ on $\Pi_\psi^\perp$. Now, in view of (4.1) by

$$\mathcal{F}_\psi(\Omega) := \left\{ u : \Omega \to \mathbb{R} \,:\, \exists C_u \text{ with } |\lambda u| \le C_u \|\lambda\|_\psi \text{ for all } \lambda \in \Pi_\psi^\perp \right\}$$

we introduce the largest among all linear spaces containing functions that allow point evaluations in the domain $\Omega \subset \mathbb{R}^d$ and on which the error functional ϵ_x is continuous for all $x \in \mathbb{R}^d$. As a result, we get the error bound

$$|s(x) - u(x)| \leq |u|_{\mathcal{F}_\psi(\Omega)} \|\epsilon_x\|_\psi$$

where the (semi-)norm $|\cdot|_{\mathcal{F}_\psi(\Omega)}$ is defined by

$$|u|_{\mathcal{F}_\psi(\Omega)} := \sup_{\lambda \in \Pi_\psi^\perp \setminus \{0\}} \frac{|\lambda u|}{\|\lambda\|_\psi} \qquad \text{for all } u \in \mathcal{F}_\psi(\Omega)$$

and $\|\epsilon_x\|_\psi^2$ comes out to be

$$\psi(0) - 2\sum_{j=0}^{M-1} v_j(x) L_j^y \psi(x-y) + \sum_{i,j=0}^{M-1} v_i(x) v_j(x) L_i^x L_j^y \psi(x-y).$$

4.1. Characterisations of native spaces. To be complete with the theoretical background, for a fixed conditionally positive definite function ψ we provide some characterisations of its corresponding function space $\mathcal{F}_\psi(\Omega)$ for which our recovery algorithm is optimal in the sense of the Holladay-theorem result. Based on earlier studies of [3], [4], [14], [15], [16], [34] among other things characterisations of the native function spaces have been surveyed in [11]. Interestingly enough, [11] proves that we do not obtain more information if we extend the definition of $\mathcal{F}_\psi(\Omega)$ to $\mathcal{F}_\psi(\mathbb{R}^d)$, since it can be shown that restriction of all functions from the latter to the domain Ω yields a function space that coincides with $\mathcal{F}_\psi(\Omega)$:

$$\mathcal{F}_\psi(\mathbb{R}^d)\Big|_\Omega = \mathcal{F}_\psi(\Omega).$$

Hence, for the description of $\mathcal{F}_\psi(\Omega)$ we can adopt the available characterisations of $\mathcal{F}_\psi(\mathbb{R}^d)$.

Theorem 4.1. *The function space $\mathcal{F}_\psi(\Omega)$ coincides with the set containing all restrictions of functions of the form*

$$u(x) = \overline{\lambda}^y \psi(x-y) + p(x), \qquad p \in \Pi_m(\mathbb{R}^d)$$

to the domain Ω, where $\overline{\lambda}$ is a functional from the closure $\overline{\Pi_\psi^\perp}$ of $\Pi_\psi^\perp$ with respect to the norm $\|\cdot\|_\psi$.

If we understand the Fourier transform $\hat{u}$ of a function u from any weighted L_2 space of the form

$$L_2(w) := \left\{ u : \mathbb{R}^d \to \mathbb{R} \,:\, \int_{\mathbb{R}^d} |u(\omega)|^2 w(\omega)\, d\omega < \infty \right\}$$

according to the Plancherel theorem we obtain the following characterisation of $\mathcal{F}_\psi(\Omega)$ which has been recognised by Wu & Schaback [34].

Theorem 4.2.

$$\mathcal{F}_\psi(\Omega) = \left\{ u : \Omega \to \mathbb{R} \,:\, \exists v : \mathbb{R}^d \to \mathbb{R} \text{ with } v\Big|_\Omega \equiv u \text{ and } |\hat{v}|/\sqrt{\varphi} \in L_2(\mathbb{R}^d) \right\}.$$

4.2. Examples. For a selection of radial basis functions we present explicit representations of their corresponding native spaces:

- As a prominent example (see [17], [18]), we consider the Beppo-Levi space

  $$BL^k(\mathbb{R}^d) := \{v \in \mathcal{D}' \mid D^\alpha v \in L^2(\mathbb{R}^d) \text{ for } |\alpha| = k\}$$

  which is equipped with the (semi-)norm

  $$|\cdot|_{BL^k(\mathbb{R}^d)} := \sqrt{\sum_{|\alpha|=k} \int_{\mathbb{R}^d} \binom{k}{\alpha} |\partial^\alpha \cdot|^2 dx}$$

  such that $\ker |\cdot|_{BL^k(\mathbb{R}^d)} = \Pi_k(\mathbb{R}^d)$ and the optimal recovery algorithm in $BL^k(\mathbb{R}^d)$ is generated by the thin plate spline:

  $$s(x) = \sum_{j=0}^{M-1} \lambda_j L_j^y |x-y|^{2k} \log(|x-y|) + v(x), \qquad v \in \Pi_k(\mathbb{R}^d).$$

- The paper [15] of Madych & Nelson provides a further example for the Gaussians $\psi(x) = e^{-\alpha|x|}$ although restricted to the univariate case $d = 1$ by

  $$\mathcal{F}_\psi(\mathbb{R}) = \left\{u : \mathbb{R}^d \to \mathbb{R} \text{ absolutely continuous } : u, u' \in L_2(\mathbb{R})\right\}$$

  which is equipped with norm $|\cdot|_{\mathcal{F}_\psi(\mathbb{R})}$ adopted from Sobolev space $W_2^1(\mathbb{R})$, which is defined by

  $$|u|^2_{\mathcal{F}_\psi(\mathbb{R})} := \frac{1}{2} \int_{\mathbb{R}} \left(|u(x)|^2 + |u'(x)|^2\right) dx \qquad \text{for all } u \in \mathcal{F}_\psi(\mathbb{R}).$$

5. Numerical results

We return to the problem of recovery of Dirac functionals from cell average data in ENO schemes.

5.1. A second-order ENO approximation. We restrict our attention to the case of two space dimensions. In that special case the finite volume approximation defined in Definition 2.7 takes the form

$$\begin{aligned}
\frac{d}{dt}\overline{u}_i(t) &= -\frac{1}{T_i} \sum_{j \in N(i)} \frac{|\partial T_i \cap \partial T_j|}{2} \sum_{\nu=1}^{2} \omega_\nu H\left(s_u^i(x_{ij}(s_\nu), t), s_u^j(x_{ij}(s_\nu), t); n_{ij}\right) \\
\overline{u}_i(0) &= \mathfrak{A}(T_i)u(0),
\end{aligned}$$

where $\overline{u}_i := \overline{u}|_{T_i}$ is used and the quadrature rule is restricted to a two-point Gaussian rule. The parametrisation of the edge $\partial T_i \cap \partial T_j$ used is $x_{ij}(s) = (x_{ij}^1 + x_{ij}^2)/2 + s(x_{ij}^2 - x_{ij}^1)/2$ if $x_{ij}^k, k = 1, 2,$ denote the two node points constituting the edge. In that case the weights are given by $s_1 = -s_2 = -0.5773502692\ldots$. A second order TVD-Runge-Kutta method according to Shu and Osher [27] is used to advance in time. Thus, the resulting method can be second order accurate in space and time.

5.2. A linear model problem. The problem to be solved is the linear model problem

$$\partial_t u + \underline{a} \cdot \nabla_x u = 0 \tag{5.1}$$

$$u(x,0) = u_0(x), \quad x \in \mathbb{R}^2 \tag{5.2}$$

with

$$\underline{a} = \begin{pmatrix} a_1 \\ a_2 \end{pmatrix} := \begin{pmatrix} \frac{1}{2} - x_2 \\ x_1 - \frac{1}{2} \end{pmatrix} \tag{5.3}$$

and

$$u_0(x) = \begin{cases} -\frac{1}{0.01}((x_1 - \frac{3}{4})^2 + (x_2 - \frac{1}{2})^2) + 1 & ; \quad (x_1 - \frac{3}{4})^2 + (x_2 - \frac{1}{2})^2 \leq 0.01 \\ 0 & ; \quad \text{else} \end{cases} \tag{5.4}$$

Thus, the initial value function is a cone of unit height the center of the base circle lying at $x = (0.75, 0.5)$. Under the influence of the partial differential equation which is a conservation law by means of the definition $f_i(u) := a_i u$ the cone is rotated around $x = (0.5, 0.5)$ such that it turns around this point completely after $t = 2\pi$. The resulting cone height and shape is measure of the accuracy and dissipativity of the numerical method used.

As a numerical flux function we use a device according to Engquist and Osher [9] which in our case takes the form

$$\begin{aligned} H^{EO}(u_l, u_r; n) &:= \left(H^+(u_l, n) + H^-(u_r, n)\right) \\ H^+(u_l, n) &:= u_l \max(\underline{a} \cdot n, 0) \\ H^-(u_r, n) &:= u_r \min(\underline{a} \cdot n, 0) \end{aligned} \tag{5.5}$$

For numerical tests three different grids are used on the unit square. Triangulation $\mathcal{T}_1^h$ is shown in figure 3 and consists of 400 points and 722 triangles. Triangulation $\mathcal{T}_2^h$ contains 2500 points and 4802 triangles and is also shown in figure 3. The third grid consists of 10000 points and 19602 triangles and is not shown for reasons of visibility. Note that the grids were generated with the aim to destroy any possible structuring of triangles. The grid generation was accomplished using the generation procedure described in [6].

5.3. Basic finite volume solutions and linear polynomial recovery. If no recovery is used, i.e. $s_u^i \equiv \overline{u}_i$, the numerical solution after a time $t = \pi$ already shows obvious signs of deterioration as can be seen in figure 4, where the results on the triangulations $\mathcal{T}_1^h$ and $\mathcal{T}_2^h$ are shown. The following table informs about the resulting cone height.

Triangulation	cone height at $t = \pi$
$\mathcal{T}_1^h$	0.188
$\mathcal{T}_2^h$	0.391
$\mathcal{T}_3^h$	0.584

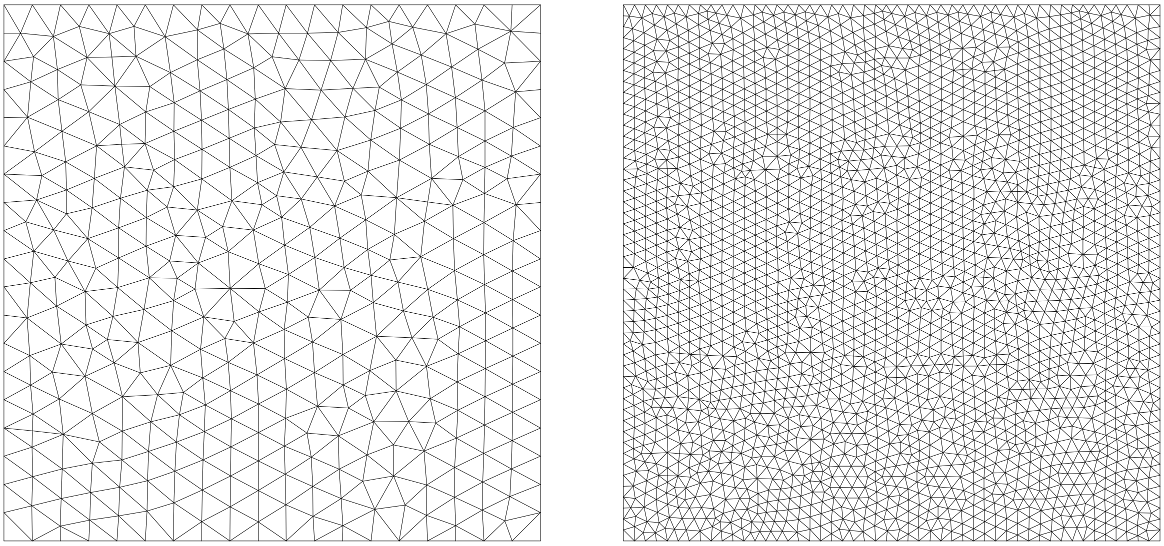

FIGURE 3. Triangulations $\mathcal{T}_{h^1}$ and $\mathcal{T}_{h^2}$

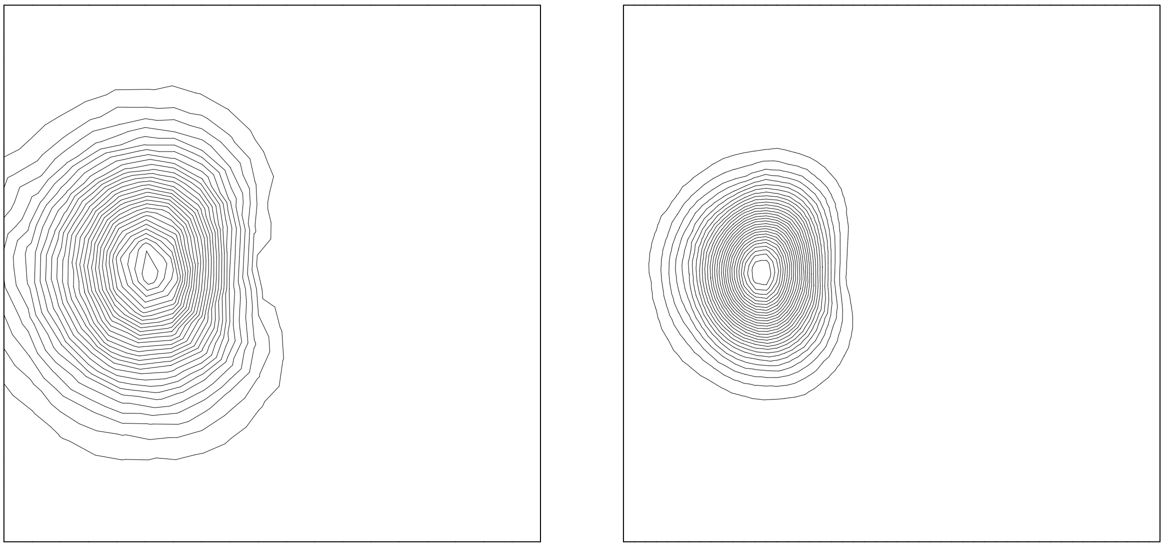

FIGURE 4. Numerical solutions without recovery on $\mathcal{T}_1^h$ (left) and $\mathcal{T}_2^h$

To demonstrate the potential of polynomial recovery we compare the results of the basic finite volume scheme with the TVD-scheme due to Durlofsky, Engquist and Osher, see [2]. Linear recovery and a limiter function is used to produce second-order accurate solutions exhibiting certain monotonicity features. The numerical solutions obtained with this scheme on triangulations $\mathcal{T}_1^h$ and $\mathcal{T}_2^h$ are shown in figure 5. For the sake of comparison

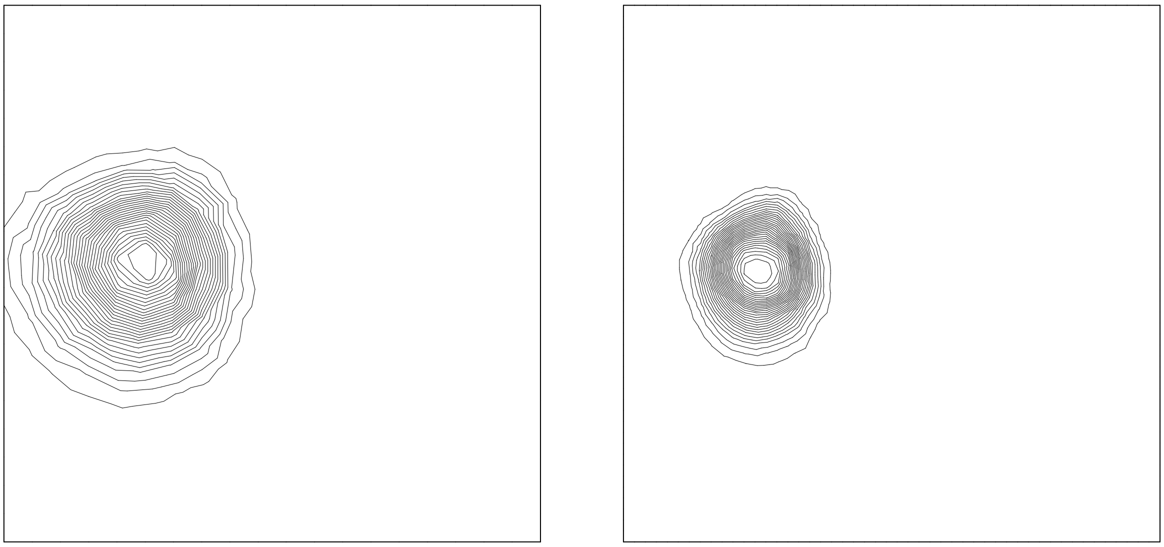

FIGURE 5. Numerical solution with TVD-scheme after Durlofsky, Engquist and Osher

the cone heights on different grids are listed again in a table.

Triangulation	cone height at $t = \pi$
$\mathcal{T}_1^h$	0.308
$\mathcal{T}_2^h$	0.678
$\mathcal{T}_3^h$	0.860

As can be seen the solution using linear recovery is much better concerning the cone height than the solutions obtained with a basic finite volume approximation. Despite this fact an inspection of the shape of the numerical solution in figure 5 shows that the surface of the cone is deformed due to the action of the limiter function.

5.4. Radial recovery. We use the stencil selection strategy as described in subsection **2.3**. On each of the four possible node sets we construct a thin plate spline

$$s_u(x) = \sum_{j=0}^{3} \lambda_j \mathfrak{A}(T_j)^y |x-y|^2 \log(|x-y|) + \sum_{\ell=0}^{2} \beta_\ell p_\ell(x)$$

with $p_0 \equiv 1$, $p_1 = x_1$, $p_2 = x_2$ according to the recovery conditions

$$\begin{aligned}
\mathfrak{A}(T_k)s_u &= \sum_{j=0}^{3} \lambda_j \mathfrak{A}(T_k)^x \mathfrak{A}(T_j)^y |x-y|^2 \log(|x-y|) + \sum_{\ell=0}^{2} \beta_\ell \mathfrak{A}(T_k) p_\ell = \overline{u}_i, \\
&\qquad k = 0, \dots, 3, \\
\sum_{j=0}^{3} \lambda_j \mathfrak{A}(T_j) p_\ell &= 0, \quad \ell = 0, 1, 2.
\end{aligned}$$

where the triangle T_i on which the recovery function is sought was again denoted with index 0 and its three members in the node set under consideration with indexes 1 - 3. While the application of $\mathfrak{A}(T_j)^y$ is approximated by the crude quadrature rule $\mathfrak{A}(T_j)^y v \approx v(x_{b_j})$, where x_{b_j} denotes the barycentre of T_j, the action of $\mathfrak{A}(T_k)^x$ is accounted for by means of a seven point quadrature rule within the triangles, compare [29].

Out of the four possible thin plate splines associated with triangle T_i we choose the one with least total variation norm $\|s_u\|_{BV(T_i)} := \|s_u\|_{L^1(T_i)} + \|\nabla s_u\|_{L^1(T_i)}$. This procedure should lead to an ENO approximation if the set of possible stencils is sufficiently rich. It turns out that four triangles in a node set are enough for these kind of model problems.

The numerical solution of the thin plate spline recovery on grids $\mathcal{T}_1^h$ and $\mathcal{T}_2^h$ is shown in figure 6. As can already be seen from the isolines the thin plate spline recovery respects

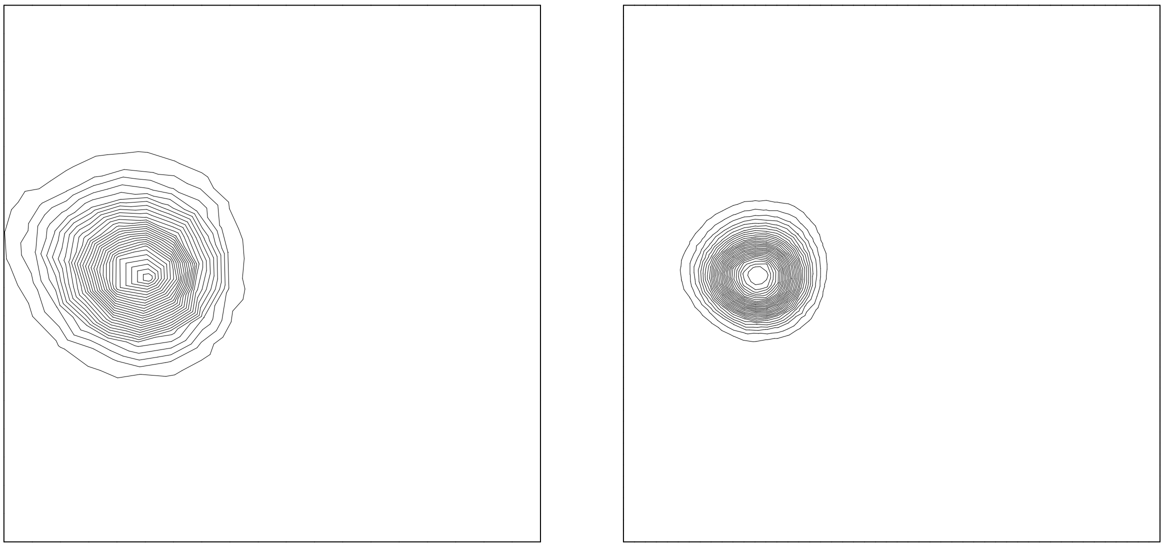

FIGURE 6. Solutions with thin plate spline recovery on grids $\mathcal{T}_{h^1}$ (left) and $\mathcal{T}_{h^2}$.

the shape of the cone much better than the linear polynomial recovery algorithm did. The resulting cone heights are given in the following table.

Triangulation	cone height at $t = \pi$
$\mathcal{T}_1^h$	0.456
$\mathcal{T}_2^h$	0.900
$\mathcal{T}_3^h$	0.975

Although these results show clearly the superiority of thin plate spline recovery the spline itself is clumsy to use in praxis due to the linear polynomial with which it is augmented. According to the table of radial basis functions given previously the Gaussian spline as well as the multiquadric and inverse multiquadric do not need any augmentation. Choosing the Gaussian spline recovery

$$s_u(x) = \sum_{j=0}^{3} \lambda_j \mathfrak{A}(T_j)^y \exp(-|x-y|^2)$$

leads to the numerical results shown in the following table.

Triangulation	cone height at $t = \pi$
$\mathcal{T}_1^h$	0.522
$\mathcal{T}_2^h$	0.989
$\mathcal{T}_3^h$	0.994

Switching to multiquadric recovery

$$s_u(x) = \sum_{j=0}^{3} \lambda_j \mathfrak{A}(T_j)^y \sqrt{1+|x-y|^2}$$

again underlines the superiority of radial recovery procedures as indicated in the following table of cone heights.

Triangulation	cone height at $t = \pi$
$\mathcal{T}_1^h$	0.520
$\mathcal{T}_2^h$	1.02
$\mathcal{T}_3^h$	1.01

Not surprising, the exponential spline as well as the multiquadric recovery gives satisfying results also with regard to the shape of the cone. For the sake of completeness the resulting numerical solutions on the fine grid $\mathcal{T}_2^h$ are shown in figure 7. As can be observed from the isolines the slight overshoots in the multiquadric recovery are not a sign of instability but an effect of the ENO reconstruction technique.

5.5. Euler's equations. In order to demonstrate the usefulness of the outlined radial recovery for problems of numerical gas dynamics we apply the recovery technique described for the linear model problem to the Euler equations, the conservative variables and fluxes of which were already given in section **2.1**. The recovery is applied to the primitive variables ρ, v_1, v_2 and p and the numerical flux function used was that of Osher & Solomon [24]. One quadrature point was used on each edge of a triangle so that the maximal order of accuracy attainable is two.

We consider supersonic flow in a channel where a step is introduced at time $t = 0$. The freestream Mach number is given by $\mathrm{Ma}_\infty = 3$ so that this case is the well-known test case of Woodward and Colella [33]. If the Euler equations are non-dimensionalised with the onflow velocity then the most interesting flow features can be seen at time $t = 8$ (this compares to $t = 4$ in [33] where the speed of sound of the onflow was used for non-dimensionalisation). A Mach stem should be seen on the upper wall of the channel from which a contact discontinuity runs downstream. A system of reflected shocks dominates the flow while the corner point of the inward pointing step gives rise to a corner singularity

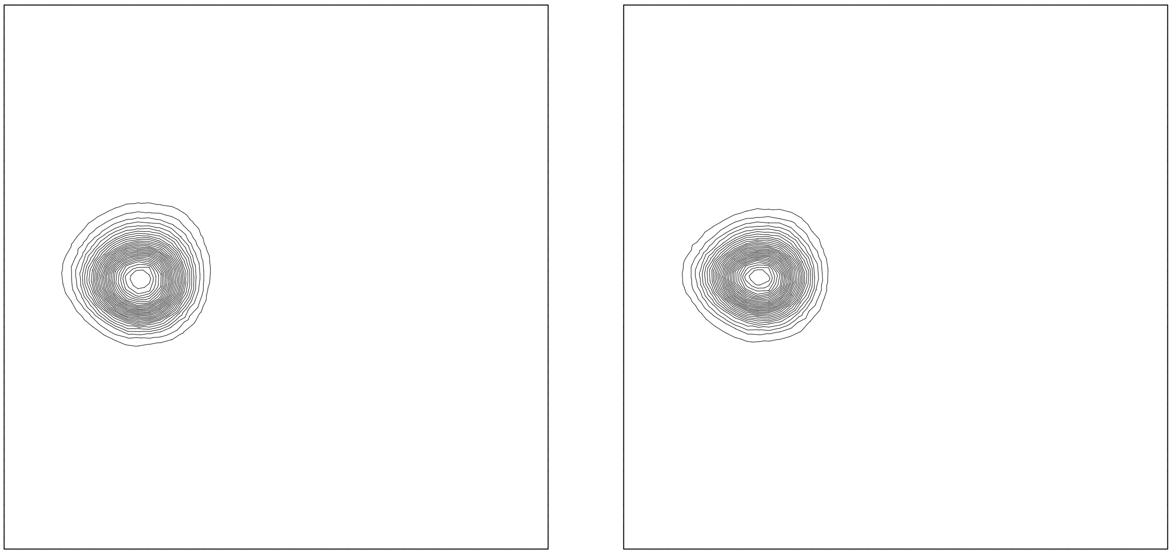

FIGURE 7. Solutions with Gaussian spline (left) and multiquadric recovery on grid $\mathcal{T}_{h^2}$.

in form of the footpoint of a rarefaction wave. The grid shown in figure 8 contains 8064

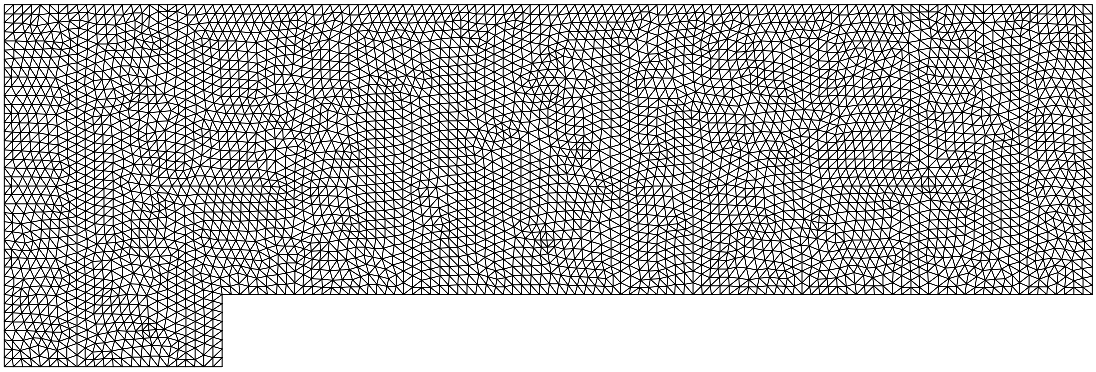

FIGURE 8. Grid for the forward facing step problem

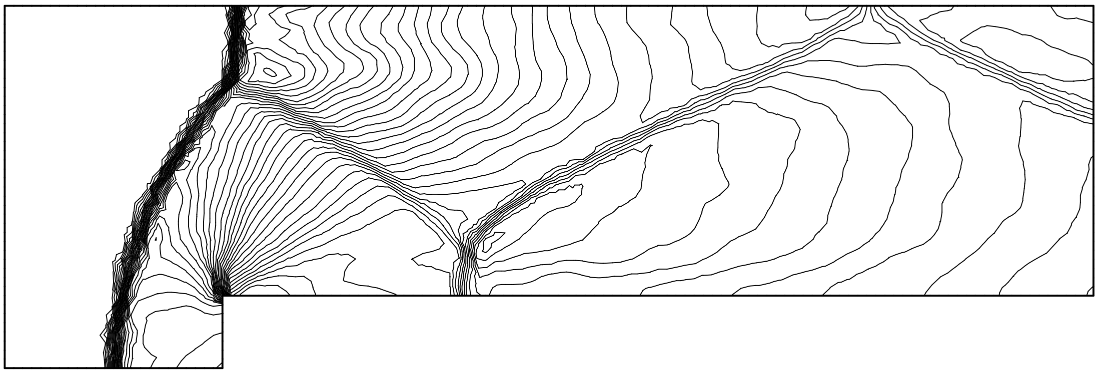

FIGURE 9. Density distribution with Durlofsky, Engquist, Osher scheme.

triangles corresponding to 4193 points. In figure 9 the density distribution of the numerical solution with the Durlofsky, Engquist, Osher scheme using linear polynomial recovery is shown and the numerical solution using the thin plate spline recovery already described in the discussion of the linear model problem computation in figure 10. As can be seen both

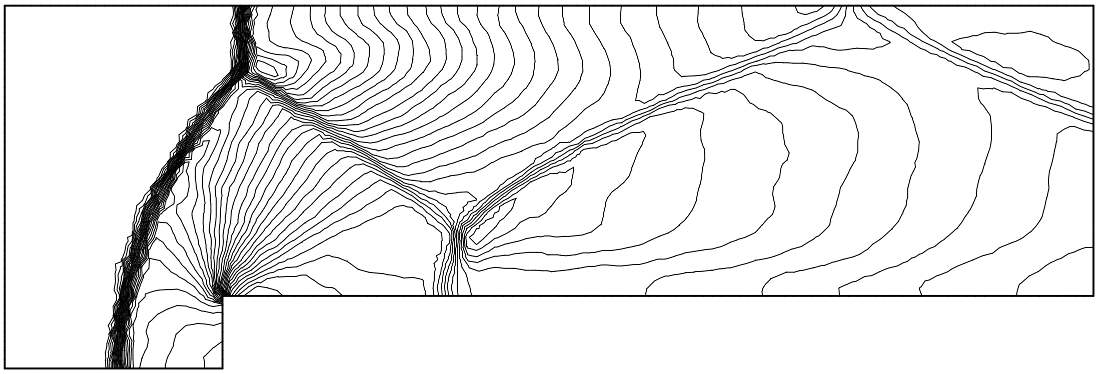

FIGURE 10. Density distribution with thin plate spline recovery.

solutions are well comparable but the thin plate spline recovery resulted in a smoother solution. Note that the contact discontinuity is slightly better resolved with thin plate spline recovery as with linear polynomial recovery.

6. Conclusions

A general theory of optimal recovery of linear functionals in native spaces of radial basis functions was developed and applied to the recovery of Dirac functionals from cell averages in the reconstruction step of finite volume ENO-approximations to hyperbolic conservation laws. Those native spaces were characterised, conditions on the recovery problem to be uniquely solvable were given and error estimates were derived. Numerical experiments have shown that radial recovery is indeed superior compared with classical polynomial recovery. The use of radial recovery functions in the numerical solution of gas dynamics problems still requires much more computation time as comparable polynomial recoveries but results in higher resolution of flow features. Future work should be directed towards the establishment of fast radial recovery algorithm to compete with polynomial recovery even in complex physical problems.

References

1. G. Bruhn - Erhaltungssätze und schwache Lösungen in der Gasdynamik. *Math. Meth. in the Appl. Sci.* ***7****, 470-479, (1985)*
2. L.J. Durlofsky, B. Engquist, S. Osher - Triangle Based Adaptive Stencils for the Solution of Hyperbolic Conservation Laws. *J. Comp. Phys.* ***98****, 64-73, (1992)*
3. N. Dyn - Interpolation of Scattered Data by Radial Functions. *Topics in Multivariate Approximation (C.K. Chui, L.L. Schumaker and F.I. Utreras, eds.). Academic Press, 47-61, (1987)*
4. N. Dyn - Interpolation and Approximation by Radial and Related Functions. in: *Approximation Theory VI: Vol. 1 (C. K. Chui, L. L. Schumaker, J. D. Ward, eds.). Academic Press, 211-234 (1989).*
5. H. Federer - Geometric Measure Theory. *Springer Verlag, Grundlehren der math. Wissenschaften Band 153, (1969)*
6. O. Friedrich - A New Method for Generating Inner Points of Triangulations in Two Dimensions. *Comp. Meth. Appl. Mech. Eng.* ***104****, 77-86, (1993)*

7. M. Golomb, H.F. Weinberger - Optimal Approximation and Error Bounds. in: *On Numerical Approximation, Edt.: R.E. Langer, The University of Wisconsin Press, Madison, (1959)*
8. A. Harten, S.R. Chakravarthy - Multi-Dimensional ENO Schemes for General Geometries. *ICASE Report No. 91-76, (1991)*
9. *C. Hirsch - Numerical Computation of Internal and External Flows, Volume 2: Computational Methods for Inviscid and Viscous Flows. John Wiley & Sons, (1990)*
10. *A. Iske - Charakterisierung bedingt positiv definiter Funktionen für multivariate Interpolationsmethoden mit radialen Basisfunktionen. Dissertation, Institut für Numerische und Angewandte Mathematik, Universität Göttingen, (1994)*
11. *A. Iske - Characterization of Function Spaces associated to Conditionally Positive Definite Functions. In: Mathematical Methods for Curves and Surfaces. M. Dæhlen, T. Lyche, and L. L. Schumaker (eds.), Vanderbilt University Press, Nashville, 1995, 265-270.*
12. *A. Iske - Reconstruction of Functions from Generalized Hermite-Birkhoff Data. In: Approximation Theory VIII, Vol. 1: Approximation and Interpolation, C. K. Chui and L. L. Schumaker (eds.), World Scientific, Singapore, 1995, 257-264.*
13. *P.D. Lax - Hyperbolic Systems of Conservation Laws and the Mathematical Theory of Shock Waves. Regional Conference Series in Applied Mathematics 11, SIAM, Philadelphia, (1973)*
14. *W. R. Madych, S. A. Nelson - Multivariate interpolation: a variational theory. unpublished preprint, 1983.*
15. *W. R. Madych, S. A. Nelson - Multivariate Interpolation and Conditionally Positive definite Functions. Approximation Theory and its Applications* **4.4** *(1988), 77-89.*
16. *W. R. Madych, S. A. Nelson - Multivariate Interpolation and Conditionally Positive definite Functions II. Mathematics of Computation, Vol. 54, No. 189 (1990), 211-230.*
17. *J. Meinguet - An Intrinsic Approach to Multivariate Spline Interpolation at Arbitrary Points. in: Polynomial and Spline Approximation, Edt.: B.N. Sahney, D. Reidel Publ. Comp., 163-190, (1979)*
18. *J. Meinguet - Multivariate Interpolation at Arbitrary Points Made Simple. ZAMP* **30***, 292-304, (1979)*
19. *C.A. Micchelli - Interpolation od Scattered Data: Distance Matrices and Conditionally Positive Definite Functions. Constr. Appr.* **2***, 11-22, (1986)*
20. *C.A. Micchelli, T.J. Rivlin - A Survey of Optimal Recovery. in: Optimal Estimation in Approximation Theory, Eds.: C.A. Micchelli, T.J. Rivlin, Plenum Press, 1-54, (1977)*
21. *C.A. Micchelli, T.J. Rivlin - Lectures on Optimal Recovery. in: Numerical Analysis, Lancaster 1984, Ed.: P.R. Turner, Springer Verlag, Lecture Notes in Mathematics 1129, 12-93, (1984)*
22. *C.A. Micchelli, T.J. Rivlin - Optimal Recovery of Best Approximations. Resultate der Mathematik* **3***, 25-32, (1978)*
23. *C. Morrey jr. - Multiple Integral Problems in the Calculus of Variations and Related Topics. Publications in Mathematics, University of California Press, Berkeley and Los Angeles, (1954)*
24. *S. Osher, F. Solomon - Upwind Difference Schemes for Hyperbolic Systems of Conservation Laws. Math. Comp.* **38***, 339-374, (1982)*
25. *M.J.D. Powell - The Theory of Radial Basis Function Approximation in 1990. Advances in Numerical Analysis II: Wavelets, Subdivision Algorithms, and Radial Basis Functions (W.A. Light, ed.). Oxford University Press, 105-210, (1992)*
26. *M. Sever - Uniqueness Failure for Entropy Solutions of Hyperbolic Systems of Conservation Laws. Comm. Pure Appl. Math.* **42***, 173-183, (1989)*
27. *- C.-W. Shu, S. Osher - Efficient Implementation of Essentially Non-Oscillatory Shock-Capturing Schemes. J. Comp. Phys.* **77***, 439-471, (1988)*
28. *J. Smoller - Shock Waves and Reaction-Diffusion Equations. Springer Verlag, Grundlehren der math. Wissenschaften Band 258, (1983)*
29. *Th. Sonar - Optimal Recovery Using Thin Plate Splines in Finite Volume Methods for the Numerical Solution of Hyperbolic Conservation Laws. submitted: IMA J. Num. Anal. (1994)*
30. *J.L. Synge - The Hypercircle in Mathematical Physics. Cambridge University Press, 1957*
31. *J.F, Traub, H. Woźniakowski - A General Theory of Optimal Algorithms. Academic Press, New York, London, Toronto, Sydney, San Francisco (1980)*

32. *P. Vankeirsbilck - Algorithmic Developments for the Solution of Hyperbolic Conservation Laws on Adaptive Unstructured Grids. Doctoral thesis, Katholieke Universiteit Leuven, Faculteit Toegepaste Wetenschappen, Afdeling Numerieke Analyse en Toegepaste Wiskunde, Celestijnenlaan 200A, 3001 Leuven (Heverlee), (1993)*
33. *P. Woodward, P. Colella - The Numerical Simulation of Two-Dimensional Fluid Flow with Strong Shocks. J. Comp. Phys.* ***54****, 115-173, (1984)*
34. *Z. Wu, R. Schaback - Local error estimates for radial basis function interpolation.* IMA Journal of Numerical Analysis ***13*** *(1993), 13-27.*

Institut für Numerische und Angewandte Mathematik, Universität Göttingen, Lotzestraße 16-18, D-37083 Göttingen

Institut für Strömungsmechanik, Abteilung Numerische Methoden, DLR Göttingen, Bunsenstraße 10, D-37073 Göttingen

E-mail address: iske@namu01.gwdg.de, Thomas.Sonar@ts.go.dlr.de